Sandia National Laboratories

Operated for the United States Department of Energy
by National Technology and Engineering Solutions
of Sandia, LLC.

Albuquerque, New Mexico 87185
Livermore, California 94550

date: May 18, 2022

to: Distribution

from: Kevin N. Long (1558) and Craig M. Hamel (1558)

subject: Stabilized Hyperfoam Modeling of the General Plastics EF4003 (3 PCF) Flexible Foam

reviewed by: Mike Neilsen (1558) and Vince Pericoli (8752)

Executive Summary

Constitutive model parameterizations for the General Plastics [5] EF4003 low density 3 pound per cubic foot are needed for design and qualification purposes in normal and abnormal mechanical simulations. The material is expected to be deformed in two ways: first during preloading, and second under impact conditions of the system (transient dynamic). All analyses are to be performed at room temperature. The goal is to provide the analysis community a robust constitutive model parameterization to represent the compression behavior of the EF4003 foam from small deformations up to massive compressive deformations when the foam is densifying. It is worth noting the EF4003 exhibits anisotropy in its stress-strain behavior between the rise and transverse directions (See figure 2.8c-d in [7]) as well as plateau behavior that is very likely to cause material stability issues, due to the buckling transition, (and has historically done so) when using Sandia's current workhorse models for flexible foams, Hyperfoam and Flex_Foam [11][13]. A Stability-informed Hyperfoam parameterization procedure is developed and executed to calibrate a hyperfoam model for the EF4003 room temperature, transversely loaded data. A rise orientation parameterization was not attempted due to localization in the experiments.

In addition to models for the full compression behavior, parameterizations are also desired that partially account for the foam preload such that analysts can approximate the response about a preloaded state without actually running the preload step. For example, if a pre-load of 35% compression is desired, we furnish constitutive model parameterizations that have the same stiffness in compression when loaded from that point, but the actual pre-loading stress is not considered. The memo lays out out what we know historically about the EF4003 foam,

the data used in this work, the hyperfoam fitting procedure employed in which model fitting is penalized to be stable (not lose ellipticity), and fitting results for both full compression curves as well as curves about different states of preload.

1 EF4003 Data

We review the background knowledge on the EF4003 foam and the compression data available for this memo. To date, previous efforts to characterize the EF4003 foam have found that the material is extremely soft, highly anisotropic, exhibits hysteresis under cyclic loading, exhibits significant damage (reduced stiffness on reloading in multiple cycles), and exhibits localization/shear banding at the macroscale when loaded at room temperature and low strain rates along the rise direction of the average pore [7, 13]. Interestingly, localization is not observed when the EF4003 foam is loaded in compression transverse to its rise direction. An example of such a deformation is reproduced from the previous references in Figure 1 for the an EF4003 specimen uniaxially loaded parallel to the bubble rise (Figure 1a) and perpendicular to the bubble rise direction (Figure 1b) at 50% nominal compressive strain.

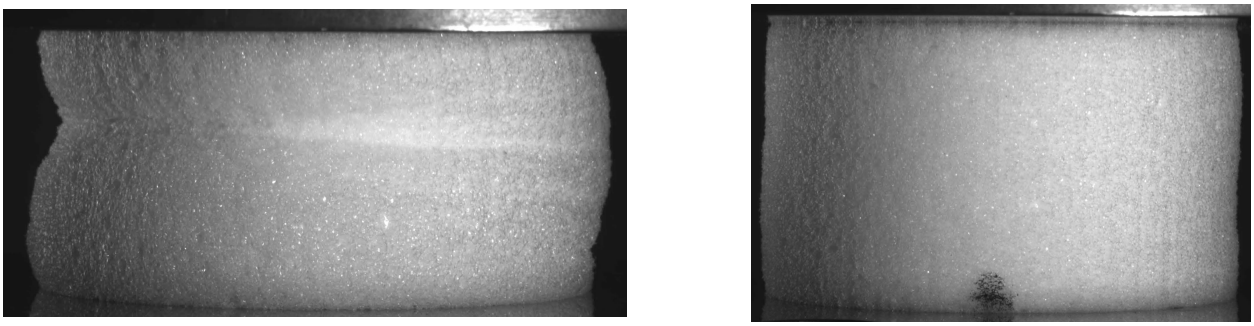

(a) Rise Loading

(b) Transverse Loading

Figure 1: Quasi-statically compressed EF4003 foam at approximately 50% nominal compressive strain [7]. (a) Loaded parallel to the bubble rise direction. (b) Loaded perpendicular to the bubble rise direction.

From [7], typical compressive stress vs. compressive strain curves as well as lateral strain vs. axial strain for loading in the transverse direction are reproduced here in Figure 2. Note that the EF4003 loaded in the rise direction does not undergo a homogenized motion, and so the nominal compressive stress vs. compressive strain curves for that direction represent structural data (specific to the 1.75 inch by 1.75 inch cylindrical specimen geometries used). Moreover, the lateral strains could not be extracted for the rise loading direction.

To measure the lateral strains using edge tracking, two orthogonal cameras were set up transverse to the loading direction, which in this case was loaded in an orientation transverse to the rise direction. Two cameras were utilized individually in a way that was identical for the one camera cases in the other foam densities reported in [7, 13]. The camera denote by "Camera 1" pointed in the direction of the bubble rise direction, while the camera denoted by "Camera 2" pointed orthogonal to the loading and the rise direction. Note that the

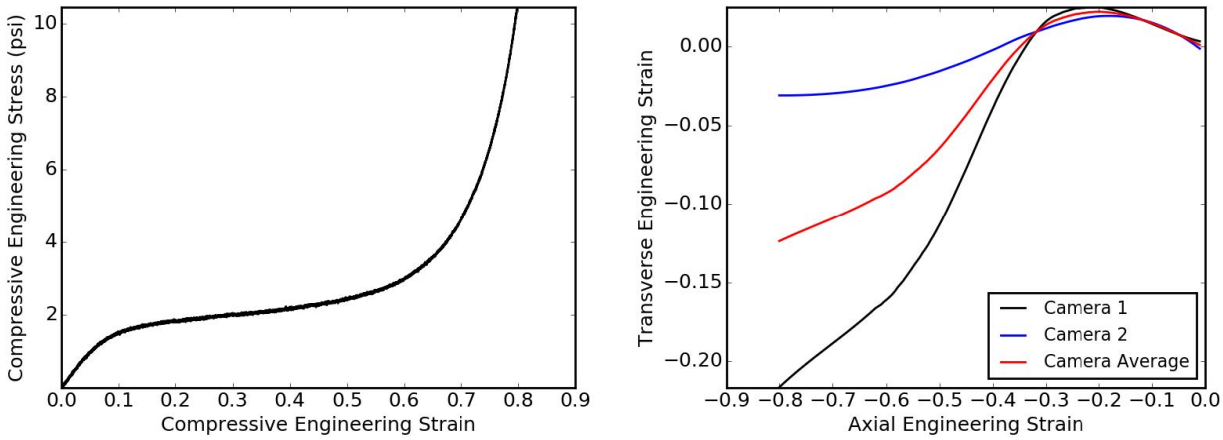

(a) Rise Loading

(b) Transverse Loading

Figure 2: Nominal compressive stress vs. compressive strain curves and lateral strain vs. axial strain from [7]. The axial strain rate used in testing was -0.01/s.

lateral strains are negative; the material is auxetic (has a negative Poisson Ratio). While other flexible foams of higher density do not show this negative lateral strain, the ordering of the rise vs. trans-trans strains are consistent with different data reduction techniques of this foam reported here [1].

Even though room temperature is well above the glass transition temperature of the TF6070 and EF4000 series foams, they exhibit some rate dependence (see [4, 2]) and damage (change in stiffness) on cyclic loading. Here, we report on prior unpublished data showing the rate dependence through cyclic loading in 2 strain rates, -0.01 and -1 per second for both rise and transverse loading in Figure 3

2 Hyperfoam Modeling

Our goal is to provide robust and accurate constitutive model parameterizations to available data in Section 1. By "Robust", we mean that the material remains stable across a broad set of deformations. Material model stability is a concern here due to the severe buckling behavior of the stress-strain curve and the fact that these foams can have structural responses when loaded in different directions. All modeling will consider the rate and temperature independent hyperfoam model [12, 14], an isotropic hyperelastic constitutive model wherein the strain energy is a function of the principal stretches of the deformation gradient. The model cannot produce damage, hysteresis due to viscoelasticity or other dissipative mechanisms, rate dependent stiffness, nor temperature dependences. However, in spite of these short falls, it is relatively easy to calibrate and check that the model parameterization remains stable over a large range of deformations. Hence, we will use this model in this work. Future work may consider the `Flex_Foam` model, which has seen successfully used for higher density flexible foams and does account for rate and temperature dependences [7, 13], but

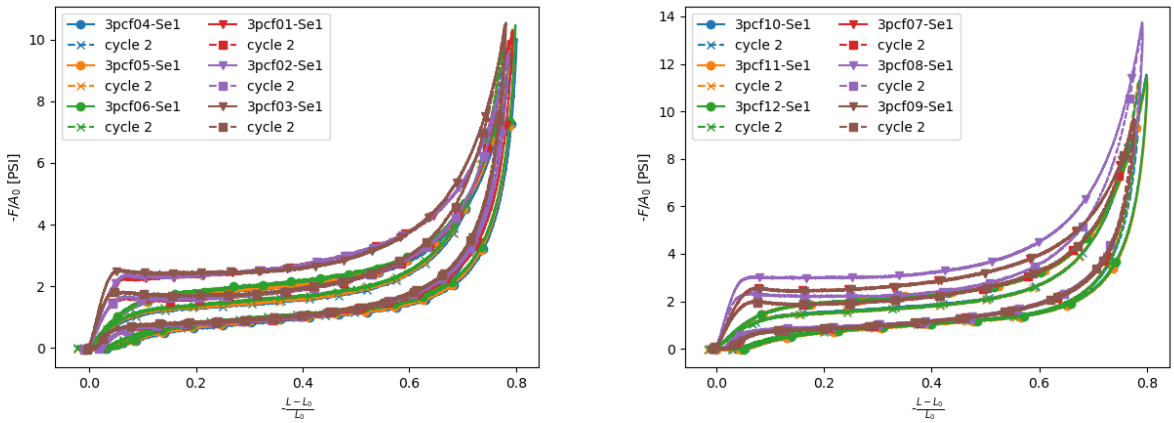

(a) 0.01 per second

(b) 1 per second

Figure 3: Cyclic compression behavior for loading in the rise and transverse directions at 2 strain rates. Note that the rise plateau is nearly flat, and the experiments visually localize. Rise data sets compose the right column in each legend while transversely loaded data sets are the left columns.

that model is harder to fully calibrate and more difficult to evaluate its stability behavior [3].

2.1 Hyperfoam Model Review and Loss-of-Ellipticity Criteria

We will use both indicial notation and direct tensor notation (through bold letters with no indices).

Reproduced directly from [12], we briefly summarize the Hyperfoam model. The strain energy density per undeformed volume is written in terms of the eigenvalues of the deformation gradient,

$$W(\lambda_k) = \sum_{i=1}^{N} \frac{2\mu_i}{\alpha_i^2} \left[\lambda_1^{\alpha_i} + \lambda_2^{\alpha_i} + \lambda_3^{\alpha_i} - 3 + \frac{1}{\beta_i} \left(J^{-\alpha_i \beta_i} - 1 \right) \right], \tag{1}$$

where μ_i and α_i are input parameters and J is the determinant of the deformation gradient. The value of β_i is calculated from the parameters ν_i via

$$\beta_i = \frac{\nu_i}{1 - 2\nu_i}. \tag{2}$$

The parameters ν_i are *initial* Poisson Ratio's for the i^{th} term, and β_i are mappings from those Poisson Ratio's that are used in the model. As a term becomes incompressible, and $\nu_i \to 0.5, \quad \beta_i \to \infty$. The lower bound for β_i is -1/3 for $\nu_i \to -1$. Note that, if different terms in the model have different ν_i, then the transverse strain behavior in uniaxial stress problems is a determined by the competing terms, and furthermore, even if the ν_i are all the same, the Poisson ratio may not be constant at finite strains. The strain energy (1) is

a sum of N contributions. The principal Kirchoff stresses for the hyperfoam model, τ_k, can be calculated as

$$\tau_k = \lambda_k \frac{\partial W}{\partial \lambda_k}, \tag{3}$$

which can be used to calculate the components of the Kirchoff stress, τ_{ij}, through

$$\tau_{ij} = \sum_{k=1}^{3} \tau_k \hat{e}_i^k \hat{e}_j^k. \tag{4}$$

where $\hat{e}_i^k$ are the components of the k^{th} eigenvector of the left stretch tensor in the global Cartesian coordinate system. Note that there is no indicial sum on the eigen index k.

With the Kirchoff stress and the deformation gradient, this relationship can be mapped to any other stress measures included the First Piola-Kirchoff stress, which is the measure used to match the uniaxial compression data and used in the stability calculations discussed next.

$$\Pi_{ij} = \frac{\partial W}{\partial F_{ij}} = \sum_{k=1}^{3} \frac{\partial W}{\partial \lambda_k} \hat{e}_i^k \bar{e}_j^k, \tag{5}$$

where $\bar{e}_j^k$ are the components of the k^{th} eigenvector of the right stretch tensor in the global Cartesian coordinate system.

Material stability calculations will require the material tangent, which is defined as the rate of change of the First Piola-Kirchoff stress, $\mathbf{\Pi}$, with respect to the deformation gradient, $\boldsymbol{F}$. For Hyperelastic materials, such as Hyperfoam, the material tangent can be calculated directly as the second derivative of the strain energy density with respect to the deformation gradient. However, it should be noted that because the strain energy density is written in terms of the principal eigenvalues of the deformation gradient, differentiation also involves the spin (rotation) of the eigenvectors of the deformation gradient.

$$\dot{\mathbf{\Pi}} = \mathbb{L} : \dot{\boldsymbol{F}} = \frac{\partial \mathbf{\Pi}}{\partial \boldsymbol{F}} : \dot{\boldsymbol{F}}, \tag{6}$$

A detailed derivation of the material tangent for the Hyperfoam model, $\mathbb{L}$, is given in [10], chapter 6.

Loss of ellipticity, or a loss of material stability, is determined when any eigenvalue of the Acoustic Tensor becomes less than or equal to zero [9, 3]. The acoustic tensor is defined through the contraction of the material tangent by an arbitrary unit direction vector, n_j,

$$A_{ik} = n_j \mathbb{L}_{ijkl} n_l. \tag{7}$$

Our condition for loss of material stability for a model calibration is when any eigenvalue of an arbitrary acoustic tensor, which is constructed in Equation 7 from the material tangent and an arbitrary unit vector, is less then or equal to zero for a motion of interest. In

practice, we do not know up front which motions our material models will be subjected to, especially in abnormal mechanical environments. Devising a sufficiently complete sampling of deformation space remains a challenge, so we pursue some simple analytic motions in the principal frame of the material point and leave more sophisticated sampling approaches to future work. Our sampling of deformation space is discussed in the algorithms below.

2.2 Hyperfoam Fitting Approach

With stability tools in hand, we describe our procedure for calibrating the Hyperfoam model for the 3PCF foam compressively loaded and checking material stability during that calibration process. Our goal is to best fit the stress-strain behavior in Figure 2 with a hyperfoam model that also does not exhibit any loss of ellipticity for any of the motions we sample. Since we will be considering rate independent and non-linear elastic modeling (no viscoelasticity and no damage), we will independently fit the loading portion of the first and second loading cycles for each of the data sets. In this way, we the fits provide a means to bound undamaged and damaged responses.

Also, for all fitting, we will consider the lateral strains to be zero rather than modeling the negative and anisotropic Poisson's ratio behavior. The choice of asserting zero transverse strain also reduces the model parameter space since all $\nu_i = \beta_i = 0$. Yet another reason to fit the data assuming zero lateral straining was because for the rise loading, where the material buckled at the specimen scale, it is not clear what the lateral strains were since the motion was not homogenous. Hence, setting the lateral strains to zero was a unique choice and a reasonable approximation.

Our Algorithm for fitting the full first loading curves of each data set is defined in Algorithm 1. Specifically, we utilize differential_evolution [6] in python's scipy library for the optimizer and we sample unit normal vectors following the spherical sampling approach outlined in [9]. Default convergence behavior for the optimizer was used.

The algorithm for checking stability is new to this work and is broken out here and presented in detail. Conceptually, using a set of material parameters from the optimizer, the suite of deformations discussed above are swept through, and for each deformation state, a suite of unit normals sampled across the unit sphere in a Cartesian sense are then swept through. For each state (6 for loops deep), the acoustic tensor is formed, and its eigenspace is examined for any values less than or equal to zero. If any are found, an unstable flag is returned, which severely penalizes the returned objective function value laid out in the Algorithm 1. The algorithm of stability checking is presented in detail in Algorithm 2.

2.3 Full Compressive Stress vs. Strain Curve Fits

The full compressive stress-strain curves associated with the loading portion of the first and second loading cycle were fit for each of the tests in Figure 3 following the procedures laid out in Algorithms 1 and 2. In all cases, the lateral strains were assigned to be zero for all deformations by assigning all $\beta_I = 0$ since we did not have lateral strains for any of

Algorithm 1 Algorithm for fitting uniaxial compression flexible foam behavior with a stability-checked Hyperfoam Model

procedure FIT COMPRESSIVE STRESS-STRAIN CURVE

Load Experimental Stress Strain Data

Define Number of Hyperfoam Terms and Bounds for Shear Moduli, Powers, and Poisson Ratios per Term

Define set of eigenvalues that two axes of principal deformation gradient will each sweep through, $\{\lambda_{1,2}\} = \{0.1, 0.3, 0.5, 0.7, 0.9, 1.0, 1.25, 1.5, 2.0, 3.0\}$

Define the set of Jacobians of the deformation gradient, that, together with $\lambda_{1,2}$ will define $\lambda_3 = J/\lambda_1/\lambda_2$. $\{\mathrm{J}\} = \{0.1, 0.3, 0.5, 0.7, 0.9,.0, 1.25, 1.5, 2.0, 3.0\ \}$.

Define the solid angle increment in normal vectors that sample the unit sphere in a Cartesian manner, which we define through an increment in each cartesian direction $dx = 0.4$ [9].

Loop through all combinations of principal stretches and Jacobians which together define a unique principal deformation gradient. Compute the material tangent, $\mathbb{L}$. Evaluate the Objective.

Define the Objective Function

Execute scipy.optimize.differential_evolution(Objective)

end procedure

procedure OBJECTIVE FUNCTION EVALUATION

Read in material parameters for each Hyperfoam term

Execute uniaxial stress calculations iterating on the lateral strains to satisfy the uniaxial stress BVP at each experimental compressive strain. See reference [8] for details and discussion on this procedure.

Obtain the L_2 norm error, e, between experimental and simulated stress-strain behavior.

Evaluate stability

if Instabilities Found **then**

Add 10^{20} to the error, e.

end if

Return e

end procedure

Algorithm 2 Algorithm for fitting uniaxial compression flexible foam behavior with a stability-checked Hyperfoam Model

procedure EVALUATE STABILITY
    Stable = True
    for λ_1 in $\{\lambda_{1,2}\}$ **do**
        for λ_2 in $\{\lambda_{1,2}\}$ **do**
            for λ_3 in $\{J\}/\lambda_1/\lambda_2$ **do**

                Compute $\mathbb{L}$

                $nrange$ = {-1, -1+dx, -1+2dx, ... 1}
                for x in $nrange$ **do**
                    for y in $nrange$ **do**
                        for z in $nrange$ **do**
                            if x, y, and z are all near zero **then**
                                Ignore This Direction
                            else
                                $N = \sqrt{x^2 + y^2 + z^2}$
                                $ex = x/N$
                                $ey = y/N$
                                $ez = z/N$
                                $\boldsymbol{n} = ex\boldsymbol{e_x} + ey\boldsymbol{e_y} + ez\boldsymbol{e_z}$

                                Compute the Acoustic Tensor, $A_{ik} = n_j \mathbb{L}_{ijkl} n_l$

                                Compute Eigenvalues of $\boldsymbol{A}$

                                if Any eigenvalue is less than or equal to zero **then**
                                    Stable = False
                                    Return Stable
                                end if
                            end if
                        end for
                    end for
                end for
            end for
        end for
    end for
    Return Stable
end procedure

the rise curves, and we cannot model anisotropy with the Hyperfoam model seen in the transverse loading experiments. Because the loading is expected to be dynamically applied in an impulse/impact scenario with higher stresses due to viscoelastic effects, we will only present the 1/s strain rate results. The cycle 1 loading at 1/s curves for the rise and transverse configurations are presented in Figure 4. The sharp plateau of the rise behavior cannot

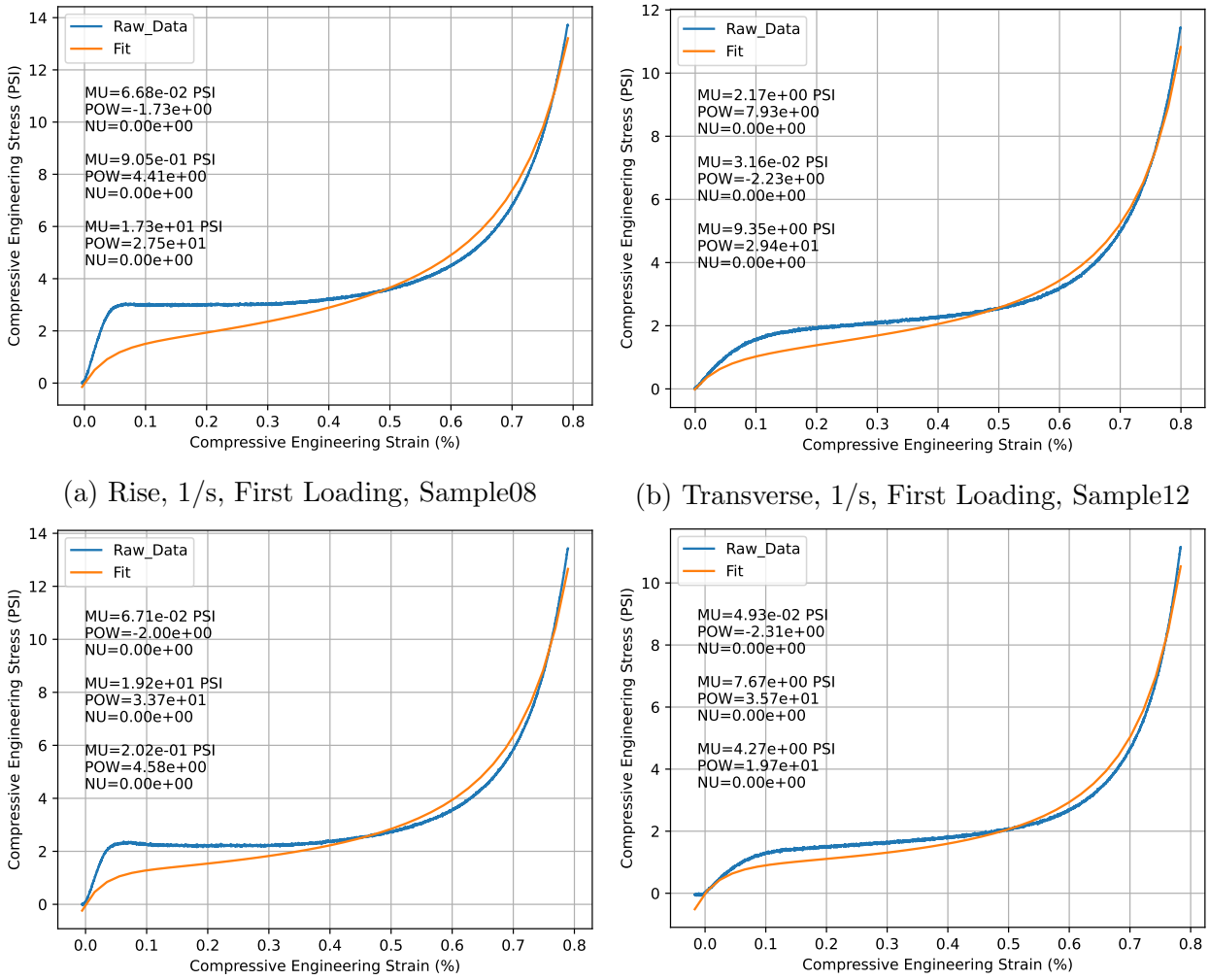

(a) Rise, 1/s, First Loading, Sample08

(b) Transverse, 1/s, First Loading, Sample12

(c) Rise, 1/s, Second Loading, Sample08

(d) Transverse, 1/s, Second Loading, Sample11

Figure 4: Three term Hyperfoam fits to rise and transversely loaded plugs of 3PCF foam.

easily be fit by the Hyperfoam model especially when unstable model parameterizations are thrown out in Algorithm 2. Even the transversely loaded curves are not well fit as they transition from linear elastic behavior to the cell buckling plateau. In all cases, densification is reasonably well modeled for the data available. Recall that the rise loading behavior is unstable experimentally with obvious localizations, so we are ignoring such details with the modeling here (which has assumed uniform motion).

2.4 Fitting behavior about the preloaded state of 35% compression

The 3PCF foam is likely the softest material in the entire system, and so, when it is loaded in series with any other material/component, it will accomodate most of the deformation. But, as we can see in the stress-strain curves for example in Figure 4, the stiffness changes considerably at different strains. Ideally, the analyst would like the ability to simulate the stiffness response of the 3PCF foam in a preloaded state without actually having to run a preloading step of the simulation. Here we present a simplified approach to modify the experimental data and fit a new hyperfoam model to a material about a preloaded state. This approach will not consider the stress in the foam, but it will get the right stiffness of the foam about the state of preload under further compression (though not if the foam is immediately unloaded in tension; that response would be incorrect).

Our procedure for creating a material parameterization to mimic the material response about a preloaded state is as follows. Given an estimated pre-strain, we shift the stress-strain curve so that the new zero stress at zero strain state is at the point where the original data was at the pre-strain/stress point. See Figure 5 for a visual aid. This approximation has a few

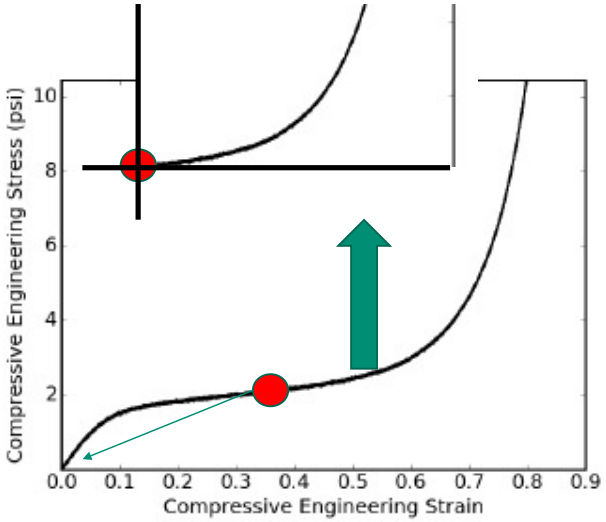

Figure 5: Shifting the data to represent the stiffness and subsequent loading behavior about the preloaded state.

negative features. The stress-free state (now in the preloaded state) is not actually stress-free in reality, which could affect normal vibration and handoff simulations to structural dynamics. Other approaches for calibrating models to a preloaded state should be considered.

The user must input the estimated preload strain, and then with this shifting procedure, the new stress-strain curve is then fit with the Hyperfoam modeling following the procedure and tools from the previous sections. For the 3PCF foam, fits were produced for the 35% preload case as shown in Figure 6. Regarding the shifted experimental curves in Figure 6, the effect of the first and second cycle of loading is negligible. Damage (loss of stiffness) appears to be concentrated at smaller strains than 35%. Indeed, there is only a small difference between

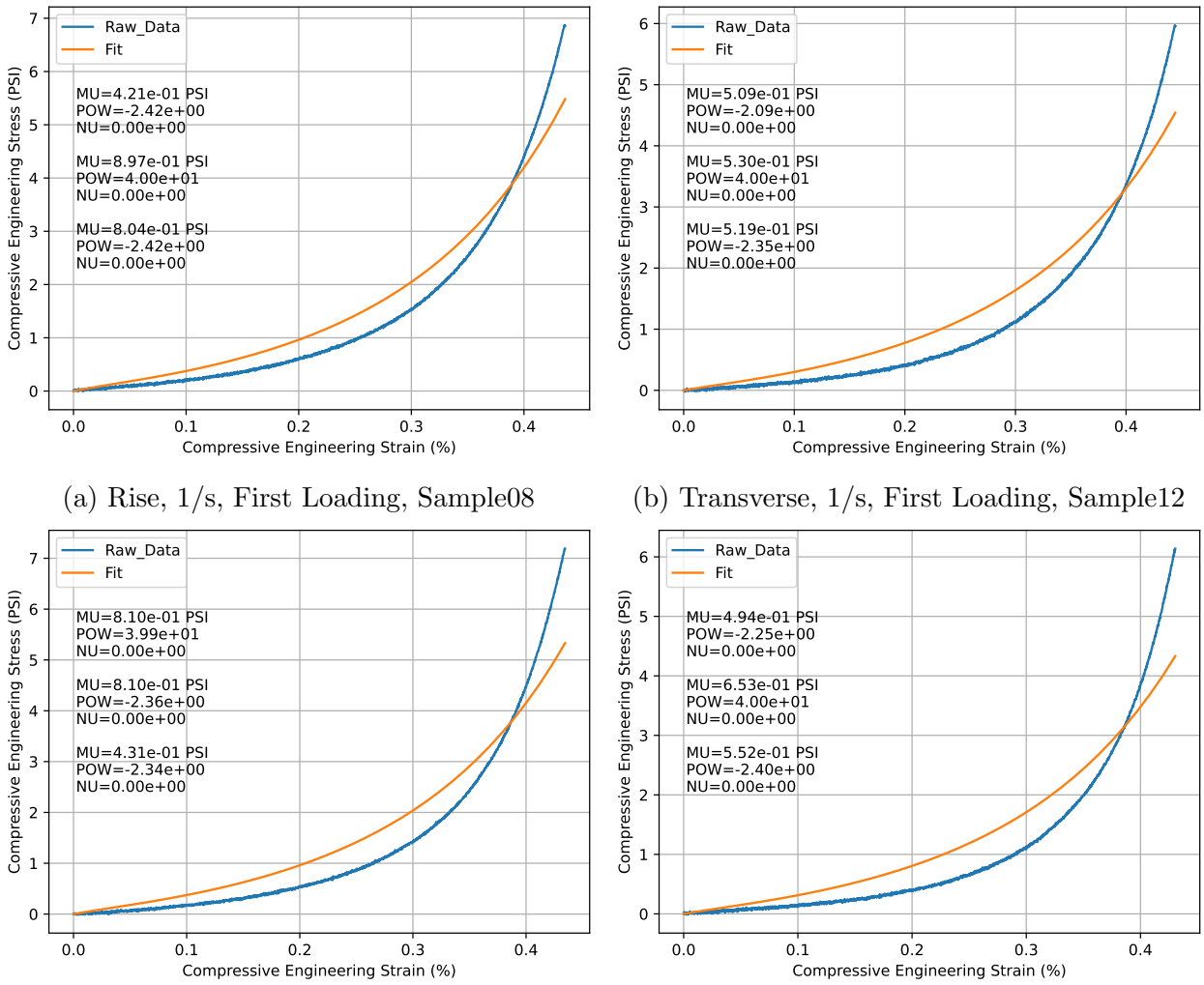

(a) Rise, 1/s, First Loading, Sample08

(b) Transverse, 1/s, First Loading, Sample12

(c) Rise, 1/s, Second Loading, Sample08

(d) Transverse, 1/s, Second Loading, Sample11

Figure 6: Three term Hyperfoam fits to rise and transversely loaded plugs of 3PCF foam after the 35% nominal compressive preload strain has been removed. I think you need to remove the % from the xlabels

the rise and transverse loading curves after this 35% preload shifting procedure is applied. The models fit the experimental curves only roughly and really do not capture the lock-up behavior. This shortcoming may be due to the stability requirement, but it is the best we were able to produce given the short timeframe of the effort.

3 Summary and Conclusions

This memo provides Hyperfoam fits for the room temperature, large deformation behavior of the EF4003 (3 PCF) foams loaded both along the bubble rise and transverse to the bubble rise directions to support large deformation, transient dynamics finite element simulations.

Cyclic compression experimental results are shown at 0.01 and 1/s for two cycles. The rise direction experiments show localized deformation (loss of homogenous motion) while the motion remained homogenous for the transversely loaded specimens. For the transversely loaded specimens, lateral strains were collected both along the rise direction and lateral to it. Lateral strains were different and negative.

The rate independent, isotropic hyperelastic Hyperfoam model was used for all fits. For all curves, a zero Poisson Ratio was considered such that the lateral strains were identically zero. The loading curves for the first and the second cycles were fit separately at each strain rate. The model does not consider viscoelasticity or damage (loss of stiffness between the two loading cycles).

A fitting procedure was developed that minimized the L_2 error between the experimental and simulated uniaxial compressive stress-strain curves subject to a severe penalty if the specific model parameterization was found to violate the strong ellipticity condition. Such a procedure generally resulted in fits of the compressive stress-strain curves that exhibited a less abrupt transition from the linear elastic regime to the cell buckling region (the plateau region) compared with the experiments. Fits are much better if stability is ignored, but stability-unaware fits have proven problematic in large finite element simulations. All fits were reasonable at large deformations where the foam is densifying. It was pointed out by the reviewers that this severe stability penalization approach may be too restrictive, and perhaps it is worth considering alternative, possibly smoother, penalizations to the objective function when loss-of-ellipticity is encountered for a particular parameter set.

A second fitting procedure was developed to model the stiffness response of the 3PCF foam about a specific state of prestrain. Such model parameterizations enable the analyst to model the foam response in a state of prestrain (as assembled in the system) without having to model the preloading step. Model fits to the modified (prestrain) data do not fit the experimental data as well as fits to the full compression stress strain curves, but they still provide a reasonable approximation for large deformation behavior. Future efforts should consider alternative ways to model pre-strained foams.

Model parameterizations are provided in the appendix.

References

[1] Dan S. Bolintineanu, Robert Waymel, Henry Collis, Kevin N. Long, Enrico C. Quintana, and Sharlotte L.B. Kramer. Anisotropy evolution of elastomeric foams during uniaxial compression measured via in-situ x-ray computed tomography. Materialia, 18:101112, 2021.

[2] Edmundo Corona. Simulation of kolsky bar tests on 15 pcf polyurethane foam. Sand2021-9204 ctf, Sandia National Laboratories, July 2021.

[3] Craig M. Hamel. Stability informed calibration approach for hypoelastic foam constitutive models. Sand2021-9060 ctf, Sandia National Laboratories, 2021.

[4] Craig M. Hamel and Kevin N. Long. Rate-dependent model calibrations of flexible polyurethane foams of various densities for the flex foam model. Sand2021-0071 ctf, Sandia National Laboratories, 2021.

[5] General Plastics (https://www.generalplastics.com/products/last-a-foam-tf 6070-series). High-density flexible foam, 2019.

[6] Eric Jones, Travis Oliphant, Pearu Peterson, et al. SciPy: Open source scientific tools for Python, 2001–.

[7] Robert Waymel Dan Bolintineanu Enrico Quintana Kevin N. Long, Craig M. Hamel and Sharlotte Kramer. Room temperature, quasi-static characterization and constitutive model parametrization of flexible polyurethane foams of different densities loaded in different orientations. SAND2020-10730 (UUR), Sandia National Laboratories, October 2020.

[8] Kevin N. Long, Doug J. Van Goethem, Brian Werner, and Nicholas Wyatt. Constitutive model calibrations for tf-6070-10 general plastics 10 pound per cubic foot flexible polyurethane foam. MEMO SAND2018-11149 R, Sandia National Laboratories, 2018.

[9] A. Mota, Q. Chen, J.W. Foulk III, J.T. Ostien, and Z. Lai. A cartesian parametrization for the numerical analysis of material instability. International Journal for Numerical Methods in Engineering, 108(2):156–180, 2016.

[10] Raymond W Ogden. Non-linear elastic deformations. Courier Corporation, 1997.

[11] William Scherzinger and Brian Lester. Library of advanced materials for engineering (lame) 4.44. UUR SAND2017-4015, Sandia National Laboratories, April 2017.

[12] William Scherzinger and Brian Lester. Library of advanced materials for engineering (lame) 4.56. UUR SAND2020-3408, Sandia National Laboratories, March 2020.

[13] D.S. Bolintineanu E. Quintana R. Waymel C.M. Hamel J. Koester A. Frankel S. A. Roberts C. Martinez B. Donohoe J. Miers T.A. Ivanoff S.L.B. Kramer, K.N. Long and H. Collis. Large-deformation mechanics of flexible polymer foams. SAND (UUR) 2021-1825, Sandia National Laboratories, February 2021.

[14] B. STORAKERS. On material representation and constitutive branching in finite compressible elasticity. JOURNAL OF THE MECHANICS AND PHYSICS OF SOLIDS, 34(2):125–145, 1986.

4 Model Parameterizations for Sierra/SM Finite Element Analysis

For all models attached, the stress units are in pounds force per square inch (PSI). The "ALPHA" and "POISSON" parameters are dimensionless.

4.1 Parameterization for the rise loading, 1/s, first cycle loading (Sample 8)

```
#####
        begin parameters for model hyperfoam
                Shear Modulus = 29.881832  # Initial Shear Modulus
                Bulk Modulus = 19.921221  # Initial Bulk Modulus
                #
                N = 3
                #
                SHEAR = 1.452e-01 8.678e+00 2.106e+01
                #
                ALPHA = -9.984e-01 3.597e+01 3.877e+01
                #
                POISSON = 0.000e+00 0.000e+00 0.000e+00
                #
        end parameters for model hyperfoam
```

4.2 Parameterization for the rise loading, 1/s, second cycle loading (Sample 8)

```
#####
        begin parameters for model hyperfoam
                Shear Modulus = 22.852317  # Initial Shear Modulus
                Bulk Modulus = 15.234878  # Initial Bulk Modulus
                #
                N = 3
                #
                SHEAR = 1.811e+01 5.304e-02 4.684e+00
                #
                ALPHA = 3.928e+01 -2.300e+00 3.089e+01
                #
                POISSON = 0.000e+00 0.000e+00 0.000e+00
                #
        end parameters for model hyperfoam
```

4.3 Parameterization for the transverse loading, 1/s, first cycle loading (Sample 12)

```
#####
        begin parameters for model hyperfoam
                Shear Modulus = 13.724517  # Initial Shear Modulus
                Bulk Modulus = 9.149678  # Initial Bulk Modulus
                #
                N = 3
                #
                SHEAR = 8.115e+00 6.479e-02 5.545e+00
                #
                ALPHA = 3.015e+01 -1.754e+00 2.010e+01
                #
                POISSON = 0.000e+00 0.000e+00 0.000e+00
                #
        end parameters for model hyperfoam
```

4.4 Parameterization for the transverse loading, 1/s, second cycle loading (Sample 11)

```
#####
        begin parameters for model hyperfoam
                Shear Modulus = 13.724517  # Initial Shear Modulus
                Bulk Modulus = 9.149678  # Initial Bulk Modulus
                #
                N = 3
                #
                SHEAR = 8.115e+00 6.479e-02 5.545e+00
                #
                ALPHA = 3.015e+01 -1.754e+00 2.010e+01
                #
                POISSON = 0.000e+00 0.000e+00 0.000e+00
                #
        end parameters for model hyperfoam
```

4.5 Parameterization for the 35% preloaded foam from rise loading, 1/s, first cycle loading (Sample 8)

```
#####
```

```
        begin parameters for model hyperfoam
                Shear Modulus = 3.144318  # Initial Shear Modulus
                Bulk Modulus = 2.096212  # Initial Bulk Modulus
                #
                N = 3
                #
                SHEAR = 1.381e+00 4.880e-01 1.275e+00
                #
                ALPHA = 3.994e+01 -2.879e+00 -2.534e+00
                #
                POISSON = 0.000e+00 0.000e+00 0.000e+00
                #
        end parameters for model hyperfoam
```

4.6 Parameterization for the 35% preloaded foam from rise loading, 1/s, second cycle loading (Sample 8)

```
#####
        begin parameters for model hyperfoam
                Shear Modulus = 3.091692  # Initial Shear Modulus
                Bulk Modulus = 2.061128  # Initial Bulk Modulus
                #
                N = 3
                #
                SHEAR = 1.256e+00 9.562e-01 8.792e-01
                #
                ALPHA = 4.000e+01 -2.743e+00 -2.393e+00
                #
                POISSON = 0.000e+00 0.000e+00 0.000e+00
                #
        end parameters for model hyperfoam
```

4.7 Parameterization for the 35% preloaded foam from transverse loading, 1/s, first cycle loading (Sample 12)

```
#####
        begin parameters for model hyperfoam
                Shear Modulus = 2.285408  # Initial Shear Modulus
                Bulk Modulus = 1.523606  # Initial Bulk Modulus
                #
```

```
                N = 3
                #
                SHEAR = 7.280e-01 7.585e-01 7.988e-01
                #
                ALPHA = -2.488e+00 -2.499e+00 3.994e+01
                #
                POISSON = 0.000e+00 0.000e+00 0.000e+00
                #
        end parameters for model hyperfoam
```

4.8 Parameterization for the 35% preloaded foam from transverse loading, 1/s, second cycle loading (Sample 12)

```
#####
        begin parameters for model hyperfoam
                Shear Modulus = 2.551853  # Initial Shear Modulus
                Bulk Modulus = 1.701235  # Initial Bulk Modulus
                #
                N = 3
                #
                SHEAR = 8.186e-01 7.228e-01 1.010e+00
                #
                ALPHA = -2.629e+00 -2.505e+00 3.996e+01
                #
                POISSON = 0.000e+00 0.000e+00 0.000e+00
                #
        end parameters for model hyperfoam
```

Internal Distribution:

MS-0845	J. Thomas	Org. 1542
MS-0840	S. Klenke	Org. 1550
MS-0840	A. Brundage	Org. 1554
MS-0840	D. Burnett	Org. 1554
MS-0840	S. Gomez	Org. 1554
MS-0346	P. Grimmer	Org. 1554
MS-0840	C. Hammeter	Org. 1554
MS-0840	D. Vangoethem	Org. 1554
MS-0346	D. Najera-Flores	Org. 1556
MS-0840	E. Corona	Org. 1558
MS-0840	E. Fang	Org. 1558
MS-0840	C. Hamel	Org. 1558
MS-0840	B. Lester	Org. 1558
MS-0840	K. Long	Org. 1558
MS-0346	M. Neilsen	Org. 1558
MS-0840	W. Scherzinger	Org. 1558
MS-0840	C. Vignes	Org. 1558
MS-9042	J. Crowell	Org. 8752
MS-9042	G. De Frias	Org. 8752
MS-9042	J. Dike	Org. 8752
MS-9042	K. Karlson	Org. 8752
MS-9042	V. Pericoli	Org. 8752